

# Modeling Regional Carbon Dioxide Flux over California using the WRF-ACASA Coupled Model

Liyi Xu, Rex David Pyles, Kyaw Tha Paw U, Shu-Hua Chen,  
Erwan Monier and Matthias Falk



Report No. 298  
June 2016

The MIT Joint Program on the Science and Policy of Global Change combines cutting-edge scientific research with independent policy analysis to provide a solid foundation for the public and private decisions needed to mitigate and adapt to unavoidable global environmental changes. Being data-driven, the Program uses extensive Earth system and economic data and models to produce quantitative analysis and predictions of the risks of climate change and the challenges of limiting human influence on the environment—essential knowledge for the international dialogue toward a global response to climate change.

To this end, the Program brings together an interdisciplinary group from two established MIT research centers: the Center for Global Change Science (CGCS) and the Center for Energy and Environmental Policy Research (CEEPR). These two centers—along with collaborators from the Marine Biology Laboratory (MBL) at Woods Hole and short- and long-term visitors—provide the united vision needed to solve global challenges.

At the heart of much of the Program's work lies MIT's Integrated Global System Model. Through this integrated model, the Program seeks to: discover new interactions among natural and human climate system components; objectively assess uncertainty in economic and climate projections; critically and quantitatively analyze environmental management and policy proposals; understand complex connections among the many forces that will shape our future; and improve methods to model, monitor and verify greenhouse gas emissions and climatic impacts.

This reprint is one of a series intended to communicate research results and improve public understanding of global environment and energy challenges, thereby contributing to informed debate about climate change and the economic and social implications of policy alternatives.

Ronald G. Prinn and John M. Reilly,  
*Program Co-Directors*

**For more information, contact the Program office:**

MIT Joint Program on the Science and Policy of Global Change

**Postal Address:**

Massachusetts Institute of Technology  
77 Massachusetts Avenue, E19-411  
Cambridge, MA 02139 (USA)

**Location:**

Building E19, Room 411  
400 Main Street, Cambridge

**Access:**

Tel: (617) 253-7492

Fax: (617) 253-9845

Email: [globalchange@mit.edu](mailto:globalchange@mit.edu)

Website: <http://globalchange.mit.edu/>

# Modeling Regional Carbon Dioxide Flux over California using the WRF-ACASA Coupled Model

Liyi Xu<sup>\*†</sup>, Rex David Pyles<sup>‡</sup>, Kyaw Tha Paw U<sup>‡</sup>, Shu-Hua Chen<sup>‡</sup>, Erwan Monier<sup>\*</sup>, and Matthias Falk<sup>‡</sup>

## Abstract

*Many processes and interactions in the atmosphere and the biosphere influence the rate of carbon dioxide exchange between these two systems. However, it is difficult to estimate the carbon dioxide flux over regions with diverse ecosystems and complex terrains, such as California. Traditional carbon dioxide measurements are sparse and limited to specific ecosystems. Therefore, accurately estimating carbon dioxide flux on a regional scale remains a major challenge.*

*In this study, we couple the Weather Research and Forecasting Model (WRF) with the Advanced Canopy-Atmosphere-Soil Algorithm (ACASA), a high complexity land surface model. Although WRF is a state-of-the-art regional atmospheric model with high spatial and temporal resolutions, the land surface schemes available in WRF lack the capability to simulate carbon dioxide. ACASA is a complex multilayer land surface model with interactive canopy physiology and full surface hydrological processes. It allows microenvironmental variables such as air and surface temperatures, wind speed, humidity, and carbon dioxide concentration to vary vertically. Carbon dioxide, sensible heat, water vapor, and momentum fluxes between the atmosphere and land surface are estimated in the ACASA model through turbulence equations with a third order closure scheme. It therefore permits counter-gradient transports that low-order turbulence closure models are unable to simulate.*

*A new CO<sub>2</sub> tracer module is introduced into the model framework to allow the atmospheric carbon dioxide concentration to vary according to terrestrial responses. In addition to the carbon dioxide simulation, the coupled WRF-ACASA model is also used to investigate the interactions of neighboring ecosystems in their response to atmospheric carbon dioxide concentration. The model simulations with and without the CO<sub>2</sub> tracer for WRF-ACASA are compared with surface observations from the AmeriFlux network.*

## Contents

1. INTRODUCTION .....	2
2. MODELS, METHODOLOGY AND DATA .....	4
2.1 Model Description .....	4
2.2 Carbon Dioxide Tracer .....	5
2.3 Data .....	6
2.4 Model Setup .....	7
3. RESULTS AND DISCUSSION .....	7
4. SUMMARY AND CONCLUSION .....	20
5. REFERENCES .....	22

---

<sup>\*</sup>Joint Program of the Science and Policy on Global Change, Massachusetts Institute of Technology, Cambridge, MA.

<sup>†</sup>Corresponding author (Email: [liyixm@mit.edu](mailto:liyixm@mit.edu))

<sup>‡</sup>Department of Land, Air, and Water Resources, University of California Davis, Davis, California, USA

## 1. INTRODUCTION

Carbon dioxide is widely recognized as a major contributor to the current climate change phenomenon. Its presence in the atmosphere intensifies the ability of the atmosphere to absorb and re-emit energy, resulting in increased surface temperatures. Although carbon dioxide is not the most efficient greenhouse gas on a molecule-to-molecule basis compared to other trace gases (such as methane or water vapor), its chemical stability, combined with its concentration and rate of increase make it the most important anthropogenic greenhouse gas to consider limiting both in the short and long-term.

Fortunately, not all anthropogenic carbon dioxide emissions contribute to increases in the global mean carbon dioxide concentration. The Global Carbon Project (2010) shows that only 47% of the anthropogenic carbon dioxide emissions from 2000 to 2009 remain in the atmosphere. Oceans uptakes accounts for about 26% of the emissions, and the remaining 27% is attributed to the terrestrial ecosystems, referred to as the ‘missing sink’ of anthropogenic carbon emissions (Wigley and Schimel, 2005). Recently compiled evidence suggests that photosynthetic bacteria in the near-surface soil horizon in recovering grasslands, bushlands, and savannah-type ecosystems account for a significant portion of the terrestrial sink (add citation 1). While this may be true, soil moisture and nutrient conditions are so widely varying that none have yet made the effort to track them with models and observations over large areas.

Though not often considered in the popular vernacular surrounding global mean concentrations, the influence of terrestrial carbon processes on seasonal timescales is visible in the atmospheric carbon dioxide concentration. The sinusoidal variation within the annual atmospheric carbon concentration is mainly due to the terrestrial growing season in the northern hemisphere, which has more land surface area than the southern hemisphere. Although it accounts for a significant amount of carbon dioxide exchange with the atmosphere and anthropogenic carbon uptake, there are large uncertainties in estimating this terrestrial carbon flux. As a result, estimates are often implicitly calculated—for example, the terrestrial carbon sink of anthropogenic CO<sub>2</sub> in the Global Carbon Project is estimated as the residual of the atmospheric carbon concentration increase and the model ocean carbon uptake. Furthermore, the latest IPCC assessment report also points out that the uncertainties in climate change may be a result of uncertainties in the carbon cycle (Collins *et al.*, 2006). Hence, quantifying the carbon dioxide flux between the atmosphere and the biosphere remains a major challenge to the climate research community.

The exchange of carbon dioxide between the terrestrial system and the atmosphere is controlled by complex spatial, temporal and plant physiological variations. The eddy covariance (EC) sensing method is widely used and regarded as the most accurate method to directly measure the carbon dioxide exchange between the atmosphere and the terrestrial system at time scales that resolve turbulence-driven variations. This EC method estimates the carbon dioxide flux through high frequency measurement of vertical wind velocity and carbon dioxide density (0.1 to 0.05 Hz). However, this method is not without problems and limitations. The EC method is most appropriate over large areas of horizontally homogeneous vegetation and flat terrain. Flux is only applicable to the area of interaction under turbulent conditions, known as the “flux footprint”. The expensive instrumentation, long periods of measurement, and extensive maintenance

and calibration requirements of the EC measurement system tend to limit the widespread adoption of carbon dioxide flux measurement. Therefore, it is difficult to assess the regional scale carbon dioxide flux between the terrestrial system and the atmosphere over a complex region such as California using only the EC method.

Typically, this limitation is alleviated by considering wider perspectives. Projects and analyses that combine remotely-sensed data and modeling simulations along with ground-based observations are both mutually supportive and useful in terms of advancing atmospheric sciences (and the STEM set) at large. In order to fill in the gaps where EC measurements are not available or applicable, numerical models have been developed to simulate the effects of land surface on climate and atmosphere conditions and to calculate carbon dioxide fluxes. These models are referred to as Land Surface Models (LSMs) or Surface Vegetation Atmosphere Models (SVATs). However, carbon dioxide exchange is excluded from many of the LSMs widely available in the field, such as the mesoscale Weather Research and Forecasting (WRF) model. LSMs with carbon calculations in climate studies differ greatly in complexity and atmosphere-biosphere interaction. For example, low complexity “big leaf” models oversimplify plant physiological processes and atmosphere-biosphere interactions (Paw U, 1997). The lack of multiple vegetation layers in a big leaf model renders it unable to resolve turbulence and vertical gradients that drive CO<sub>2</sub> fluxes (Wohlfahrt *et al.*, 2001; Baldocchi and Meyers, 1998). Thus, they tend to overestimate CO<sub>2</sub> uptake by plants as suggested by Paw U (1997). The development and usage of high complexity models that include representations of different vegetation covers, multiple canopy layers and interactive physiological processes are crucial in estimating carbon sequestration and energy balances, all of which are important components of the climate system (Potter *et al.*, 1993; Sagan and Khare, 1979; Anthes, 1984; Bougeault, 1991; Mihailovic *et al.*, 1993). Furthermore, the importance of the terrestrial carbon sink is not limited to its amount of carbon uptake. Spatial and temporal distributions of the carbon sources and sinks have increasingly been the topic of discussion. Examples of this discussion include numerous studies from the AmeriFlux network using eddy covariance methods, which have shown that terrestrial carbon sinks vary in time, location, and weather conditions (Baldocchi *et al.*, 2001; Falge *et al.*, 2002; Law, 2007). Thus, estimating the distribution of carbon is crucial in understanding the mechanisms and sustainability of the current terrestrial carbon sink.

In this study, the atmosphere-biosphere carbon dioxide exchange over the complex region of California is investigated using the mesoscale Weather and Research Forecasting model (WRF) coupled with the high complexity land surface model Advanced Canopy-Atmosphere- Soil Algorithm (ACASA), which is developed in UC Davis. In addition to simulating the carbon fluxes between the two systems, the WRF-ACASA coupled model also changes the atmospheric carbon dioxide concentration according to terrestrial carbon production/sequestration and atmospheric carbon transport via spatial advection. Therefore the coupled model is capable of tracking the atmospheric carbon dioxide concentration to identify combined impact of spatial and temporal variations of carbon sources and sinks of regional scale, along with their feedbacks. With all the tools in place, the objectives of this study are to (1) quantify the biosphere-atmosphere exchange of carbon dioxide on a regional scale and (2) investigate the effect of atmospheric interactions

between the adjacent ecosystems on the plant physiological processes at local and regional scales.

## 2. MODELS, METHODOLOGY AND DATA

### 2.1 Model Description

The WRF model is a state-of-the-art mesoscale weather model developed for both operational forecasting and atmospheric research. The model physics and dynamic features include an Eulerian solver for the fully compressible non-hydrostatic equations with mass vertical coordinates, third-order Runge-Kutta time-integration, and fully conservative flux divergence integration. The high spatial and temporal resolution is ideal for studying the complex region of California. However, because its default land surface models are relatively simplistic and none of them simulate carbon dioxide, the microscale land surface model ACASA is introduced as a submodel of WRF.

ACASA represents the interaction between vegetation, soil, and the atmosphere based on physical and biological processes described at the leaf or field scale (microscale). It is a complex multilayer analytical land surface model that simulates both the microenvironment profiles and turbulent exchanges of energy, mass and momentum within the surface-layer. The surface layer is represented as multiple vertical layers within and immediately above the canopy into the lowest planetary boundary layer, the “surface sub-layer” or “constant flux layer”. The model also incorporates the higher third order turbulent closure scheme based on Meyers and Paw U (1986) and Meyers and Paw U (1987) to allow turbulent kinetic and thermodynamic processes to transport energy, mass, and carbon fluxes in both down-gradient and counter-gradient directions, which many lower-order models are unable to directly simulate. Surface processes such as moisture, heat, momentum, and carbon dioxide fluxes are calculated for each of the interactive layers and integrated to represent the canopy level. In addition to the turbulent processes, the fourth-order technique from Paw U and Gao (1988) is used in the model to calculate the non-linear energy budget and surface energy temperature.

Carbon dioxide flux within the model is calculated from a combination of the Ball-Berry stomatal conductance (Leuning, 1990; Collatz *et al.*, 1991) and the Farquhar *et al.* (1982) photosynthesis equation:

$$g_{s,w} = m \frac{A_n}{c_s} r h_s + b \quad (1)$$

$$r h_s = \frac{g_b q_A + g_{s,w} q_s(T_L)}{g_b + g_{s,w} q_s(T_L)} \quad (2)$$

$$c_s = c_A - \frac{A_n}{g_b} \quad (3)$$

$$A_n = V_c - 0.5V_0 - R_d = \min(A_R, A_E) - R_d \quad (4)$$

$$V_c - 0.5V_0 = \min(W_c, W_j)\left(1 - \frac{\Gamma}{C_i}\right) \quad (5)$$

where  $g_{s,w}$  is the leaf stomatal conductance to water vapor,  $A_n$  is the net  $\text{CO}_2$  uptake rate at the leaf surface,  $c_s$  and  $rh_s$  are the  $\text{CO}_2$  concentration and the fractional relative humidity at the leaf surface,  $m$  and  $b$  are empirical regression coefficients;  $c_A$  is the  $\text{CO}_2$  concentration in air,  $q_s(T_L)$  is saturated mixing ratio of water vapor at leaf temperature  $T_L$ ,  $g_b$  is the leaf boundary layer conductance,  $q_A$  is the mixing ratio of water vapor in the air,  $V_c$ ,  $V_0$  and  $R_d$  are the carboxylation, oxygenation (photorespiration) and dark respiration rates of  $\text{CO}_2$  exchange between the leaf and the atmosphere (in  $\mu\text{mol m}^{-2} \text{s}^{-1}$ ),  $A_R$  is the Rubisco activity limit of  $\text{CO}_2$  assimilation rate at lower intercellular  $\text{CO}_2$  concentration when ribulose biphosphate (RuBP) is saturated,  $A_E$  is the  $\text{CO}_2$  assimilation rate when the whole chain electron transport limits RuBP regeneration;  $W_c$  and  $W_j$  are the rates of carboxylation when RuBP is, respectively, saturated and limited by electron transport (in  $\mu\text{mol m}^{-2} \text{s}^{-1}$ ),  $\Gamma$  is the  $\text{CO}_2$  compensation point in the absence of dark respiration and  $C_i$  is the intercellular  $\text{CO}_2$  concentration (in  $\mu\text{mol m}^{-3}$ ).

Because carbon fixation and respiration vary significantly across vegetation types, the ACASA model requires meteorological inputs and additional species-specific physiological parameters (e.g. leaf area index; maximum rates of carboxylation; biochemical photosynthetic coefficients). As long as these physiological parameters can be provided or estimated, this requirement allows ACASA to couple with WRF and calculate carbon flux to and from any vegetation cover. More details on the stand-alone ACASA model can be found in Pyles (2000) and Pyles *et al.* (2000). The ACASA model has been successfully applied to the Wind River Canopy Crane site, an AmeriFlux site near Skamania, Washington, with a full set of eddy-covariance measurements that includes  $\text{CO}_2$  flux (see Paw U *et al.*, 2004, for a site description). The ACASA model has been also applied and tested in a spruce forest site in Germany (Staudt *et al.*, 2010) and a Mediterranean maquis ecosystem in Italy (Marras *et al.*, 2011). All three studies have shown that the ACASA model agrees well with surface observations of energy, moisture, and carbon dioxide fluxes.

## 2.2 Carbon Dioxide Tracer

In addition to examining the atmosphere-biosphere carbon dioxide exchange, the WRF-ACASA model is also used to investigate the interaction of carbon dioxide between neighboring regions in California. Because physiological processes vary across different land cover types and growing seasons, the carbon uptake or emissions of one land cover should impact other regions. However, these interactions are difficult to determine since traditional in-situ carbon studies are limited to small areas with homogeneous land cover types. A carbon dioxide tracer is introduced to the WRF model. The new  $\text{CO}_2$  tracer transports carbon dioxide (simulated through the surface plant physiological process) in the atmosphere, and modifies the atmospheric  $\text{CO}_2$  concentration. Consequently, variations in  $\text{CO}_2$  concentration driven by ecosystem exchanges in one region can induce interactions down-wind and between neighboring regions and biomes.

The carbon dioxide tracer uses the same physics as those used for moisture in the MRF boundary layer model, but without chemical reactions and phase changes (Hong and Pan, 1996). This moisture transport scheme has been well used and tested within the WRF model. The model is initialized with a background atmospheric carbon dioxide concentration of 385 ppm. It is then changed through biosphere-atmosphere exchange of carbon dioxide from plant physiological processes in time and space. Like other atmospheric variables WRF represents, the atmospheric CO<sub>2</sub> concentration is calculated using a terrain-following hydrostatic pressure vertical coordinate. These vertical sigma coordinates are normalized hydrostatic pressure levels derived between surface pressure and a constant upper atmosphere pressure (Laprise, 1992; Klemp *et al.*, 2003).

### 2.3 Data

The WRF-ACASA coupled model simulation produced carbon dioxide concentration and exchange estimates for all of California's geographic regions with various complex ecosystems and climate variations. Many characteristic ecosystems in California (chaparral, agricultural crops, Central Valley grassland, woodland, conifer forest, and steppe) are included. The extensive topographic and vegetation variability in California provides a great opportunity to study the interactions of neighboring land cover types and their effects on carbon flux. The climate in the region is mostly Mediterranean—summer is warm and dry, while winter is cool and moist.

There are six Ameriflux Network Eddy Covariance stations in California that are available to evaluate the WRF-ACASA coupled model over the simulation period of 2005 and 2006 (see Fig. 1). Due to the model's horizontal resolution, the Vaira Ranch and the Tonzi Ranch stations share the same model grid cell; however, the surface characteristics differ considerably. The model also assumes that each grid cell is horizontally homogeneous, and so the Vaira Ranch vegetation growing season of Oct-May is not accurately represented. The three Sky Oak sites are all located in a single grid cell over Southern California. Consequently, carbon dioxide flux simulations from the WRF-ACASA model are compared to the carbon flux measurements from these sites over different vegetation covers.

Comparing model simulations and surface observations is challenging due to the differences in heights and land covers between the observational stations and model grid points. As a result of this land-type registration issue, the Plant Functional Types (PFTs) used in the WRF-ACASA simulations can sometimes match poorly with the observed PFT at the sites (Table 1). Previous chapters show that the land cover type is an important component of the surface representation in land surface models, especially high complexity land surface models such as ACASA. Therefore, the mismatch of PFT in the WRF-ACASA coupled model is an initial condition error that negatively impacts the plant physiological simulations. When the PFTs in the WRF-ACASA coupled model agree with the observed PFT, the simulated carbon dioxide exchange improved, as will be shown in this paper. Within the framework of numerical modeling experience, though desired, this type of result is not assured in advance.



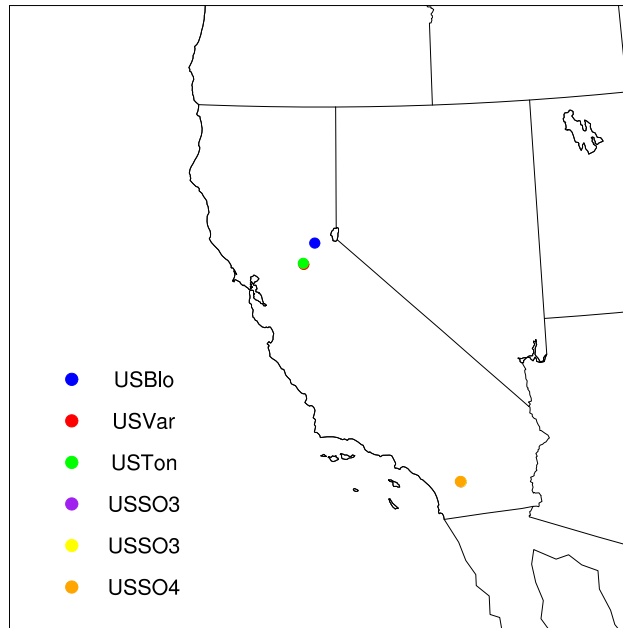


**Figure 1.** Locations of the six AmeriFlux sites used in this study. In Northern California, Blodgett Forest site is northeast of the Tonsi and Vaira sites (shown as one point). The three Sky Oak sites are closely located within the same WRF grid cell, therefore only one site is visible on the map.

## 2.4 Model Setup

Two WRF-ACASA simulations are compared: (1) WRF-ACASA with constant atmosphere carbon dioxide concentration at 385 ppm, and (2) WRF-ACASA with CO<sub>2</sub> transport in the atmosphere using the new CO<sub>2</sub> tracer. Simulations are forced by the Moderate Resolution Imaging Spectroradiometer (MODIS) LAI dataset and the Northern America Regional Reanalysis (NARR) dataset for surface and meteorological conditions to drive the initialization and boundary conditions of the WRF models (Mesinger *et al.*, 2006). Year 2005 and 2006 are simulated over California at an 8 km x 8 km horizontal resolution. Each run contains 13 months of simulations with the first month being discarded as spin-up. For example, year 2006 is simulated from December 2005 through December 2006. Atmospheric physics schemes used in this study are the Purdue Lin *et al.* scheme for microphysics (Chen and Sun, 2002), the Rapid Radiative Transfer Model for long wave radiation (Mlawer *et al.*, 1997), the Dudhia scheme for shortwave radiation (Dudhia, 1989), the Monin-Obukhov Similarity scheme for surface layer physics of non-vegetated surfaces and the ocean (Monin and Obukhov, 1954), and the MRF scheme for the planetary boundary layer (Hong and Pan, 1996). Results presented here are mostly from year 2006 because of the large amount of missing observational data in 2005.

## 3. RESULTS AND DISCUSSION

The diurnal patterns of carbon dioxide flux simulated by the WRF-ACASA model with or without varying atmospheric CO<sub>2</sub> concentration are shown in Fig. 2 and 3. Both WRF-ACASA simulations have good agreements with the surface observations when plant functional types (PFT) match between the surface observation and model. Observed diurnal patterns are created

**Table 1.** Information on AmeriFlux Stations are compared between the observation sites and the model assumptions.

Station	Site Name	WRF PFT	WRF-ACASA Canopy height (meter)	Observed height (meter)	Observed PFT
USBLO	Blodgett Forest	Evergreen Needleleaf Forest	17	12.5	Evergreen Needleleaf Forest
USVAR	Vaira Ranch	Savanna	10	1	Grassland
USTON	Tonzi Ranch	Savanna	10	23	Woody Savannas
USSO2	Sky Oak Old	Evergreen Needleleaf Forest	17	4.2	Woody Savannas
USSO3	Sky Oak Young	Evergreen Needleleaf Forest	17	1	Closed Shrublands
USSO4	Sky Oak New	Evergreen Needleleaf Forest	17	1.5	Closed Shrublands

only from days with complete 24-hour data. As pointed out in previous chapters, accurate surface representation is important for a land surface model, especially with the high complexity models such as WRF-ACASA. Both simulations perform well over the Blodgett Forest and the Tonzi Ranch, where PFTs match between observation and model. The simulated diurnal patterns of CO<sub>2</sub> flux over the Blodgett Forest and Tonzi Ranch sites are well within the one standard deviation of the surface measurements. This shows that the complex plant physiological processes in the WRF-ACASA model are robust and able to simulate the CO<sub>2</sub> fluxes correctly across the region. Although the WRF-ACASA model overestimates the CO<sub>2</sub> exchange at the three Sky Oak sites and Vaira Ranch, these flux problems are due to the input biases of PFT mismatch and lack of heterogeneous surface representation. Improvement of these surface representations will improve the WRF-ACASA simulations.

The scatter plots of hourly CO<sub>2</sub> flux (FCO<sub>2</sub>) are shown in Fig. 4 for the WRF-ACASA simulations without and with CO<sub>2</sub> tracer over the AmeriFlux sites for 2006. Both WRF-ACASA simulations compared well with the surface observations, except for the Vaira Ranch during warm months of summer and autumn, when the site vegetation is dormant due to summer drought. There are no significant differences between the two simulations from the scatter plots. The statistical analysis, however, shows that the WRF-ACASA simulation with CO<sub>2</sub> tracer reduces the Root Mean Square Error (RMSE) values for almost all stations and all seasons (Table 2).

Figures 2, 3 and 4, along with Table 2, illustrate a positive impact of varying atmospheric CO<sub>2</sub> concentration on plant physiological processes. This positive impact mainly occurs during the daytime when plants are most active. Photosynthesis by plants reduces the ambient CO<sub>2</sub> concentrations, and new CO<sub>2</sub> is transported to the site through the atmosphere. When less CO<sub>2</sub> is available in the atmosphere, photosynthetic uptake of carbon by plants is reduced. As a result, when no tracer is used and the ambient CO<sub>2</sub> concentration is held constant at 385 ppm, we can reduce the overestimation of photosynthesis and RMSE values (Table 2). For example, the diurnal CO<sub>2</sub> flux for the Blodgett forest improves during the spring, summer, autumn of 2005 and spring and

autumn of 2006 with a CO<sub>2</sub> tracer (Fig. 2 and Fig. 3).

The time series of net ecosystem CO<sub>2</sub> exchange (NEE) for each of the AmeriFlux sites during the years 2005 and 2006 display the overall ecosystem physiological activities (Fig. 5 and Fig. 6). NEE is the cumulative net primary production of carbon minus respiration, and it is calculated as the cumulative sum of carbon flux throughout the year. When NEE at the site is positive at the end of the year, the site is a carbon source, i.e. more carbon is released into the atmosphere than is absorbed; a negative annual NEE indicates an annual carbon sink.

As expected for the Blodgett Forest in 2006, the usage of a CO<sub>2</sub> tracer generally reduces the overestimation and improves the simulation of annual NEE. For example, the WRF-ACASA model with CO<sub>2</sub> tracer simulation of NEE (-930 gC m<sup>-2</sup> yr<sup>-1</sup>) closely followed the observed NEE

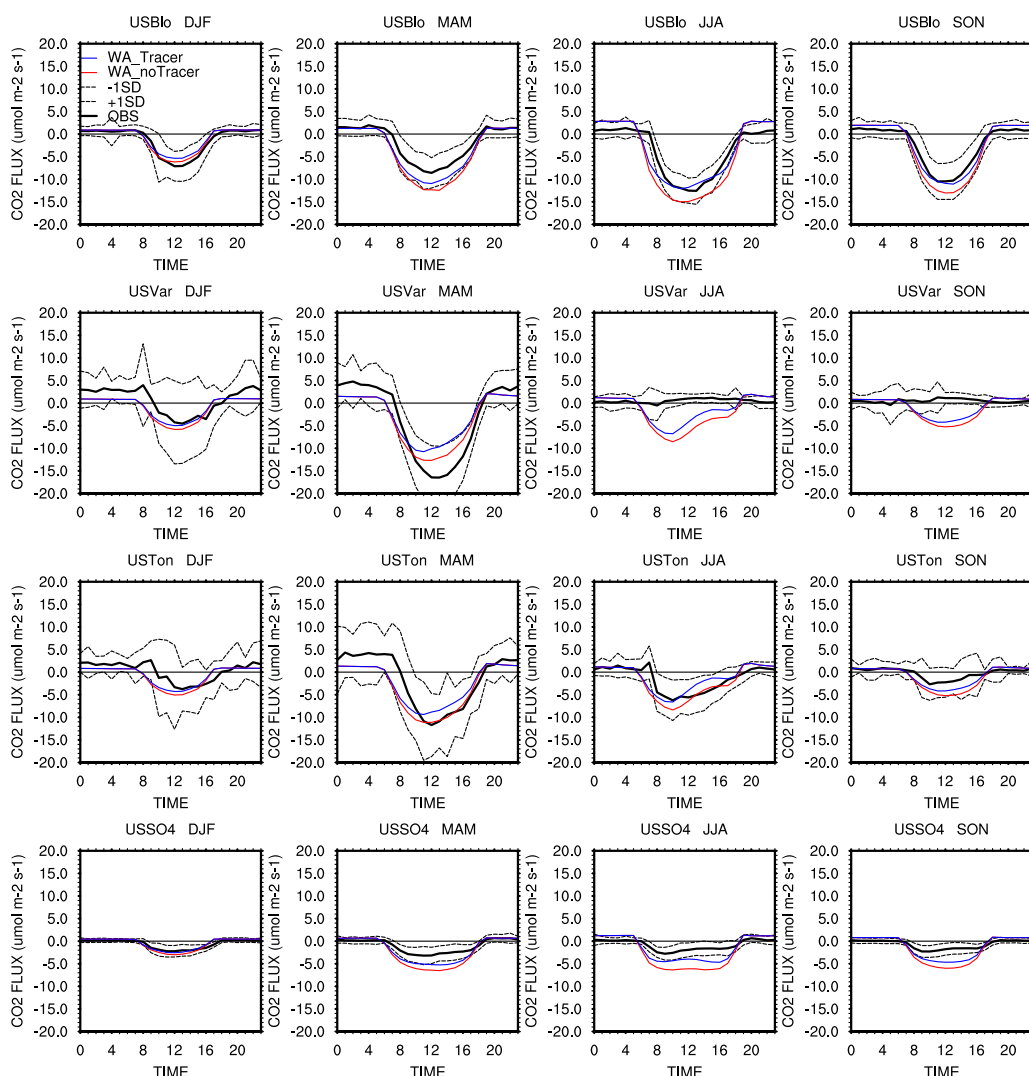


**Figure 2.** Diurnal patterns of carbon dioxide flux for the AmeriFlux sites for year 2005 by seasons. The solid black line is observation, with the dash lines representing 1 standard deviation. Blue line is WRF-ACASA with CO<sub>2</sub> tracer module, and the red line is WRF-ACASA without CO<sub>2</sub> tracer. Winter is December, January, February (DJF). Spring is March, April, May (MAM). Summer is June, July, August (JJA). And fall is September, October, November (SON).

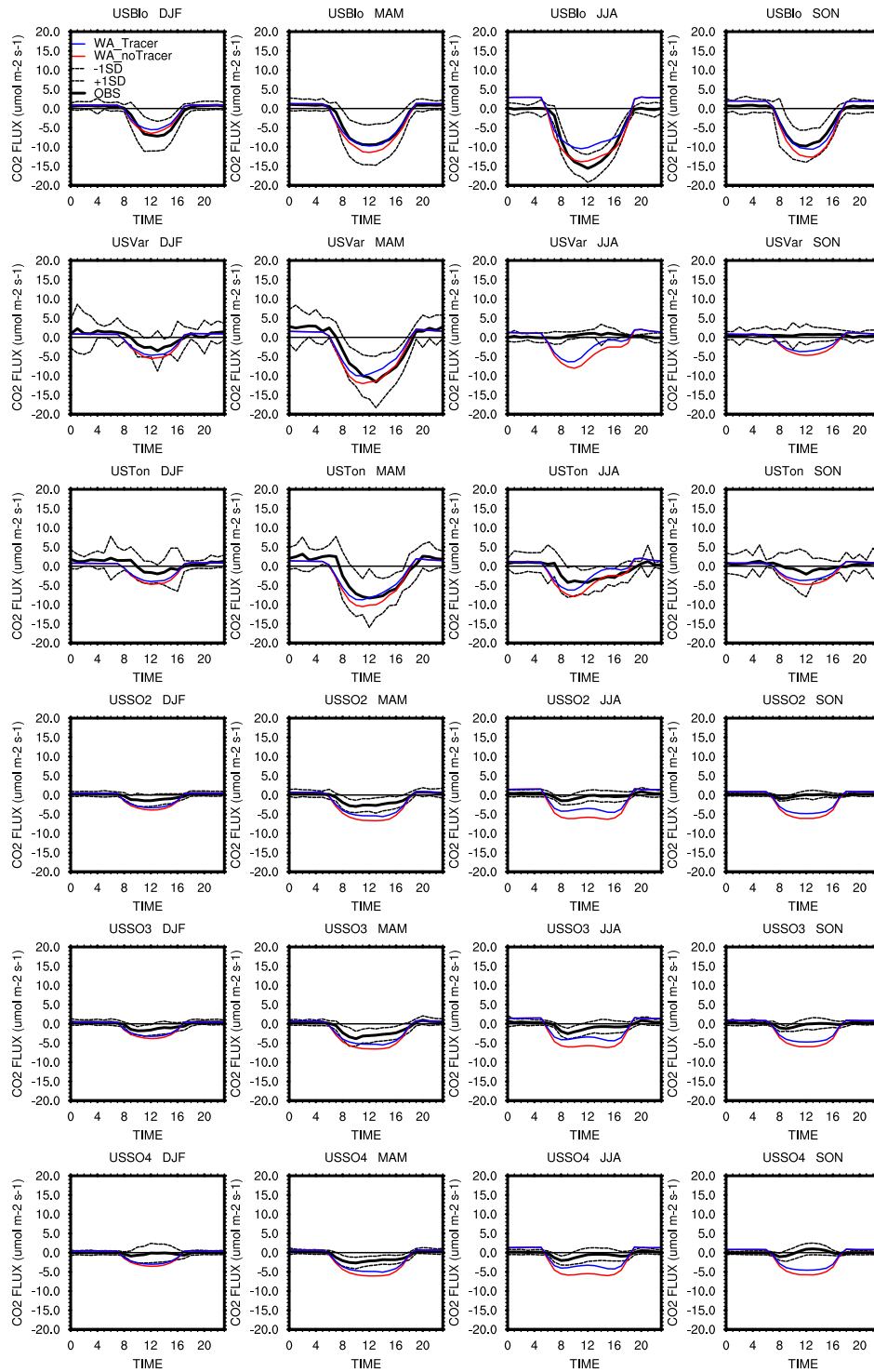


**Figure 3.** Diurnal patterns of carbon dioxide flux for the AmeriFlux sites for year 2006 by seasons. The solid black line is observation, with the dash lines representing 1 standard deviation. Blue line is WRF-ACASA with CO<sub>2</sub> tracer module, and the red line is WRF-ACASA without CO<sub>2</sub> tracer. Winter is DJF. Spring is MAM. Summer is JJA. And fall is SON.

(-908 gC m<sup>-2</sup> yr<sup>-1</sup>) for the Blodgett forest throughout year 2005 (Fig. 5, Fig. 6 and Table 3). And the CO<sub>2</sub> tracer simulated NEE for Tonzi Ranch site was -529gC m<sup>-2</sup> yr<sup>-1</sup>, comparing well with

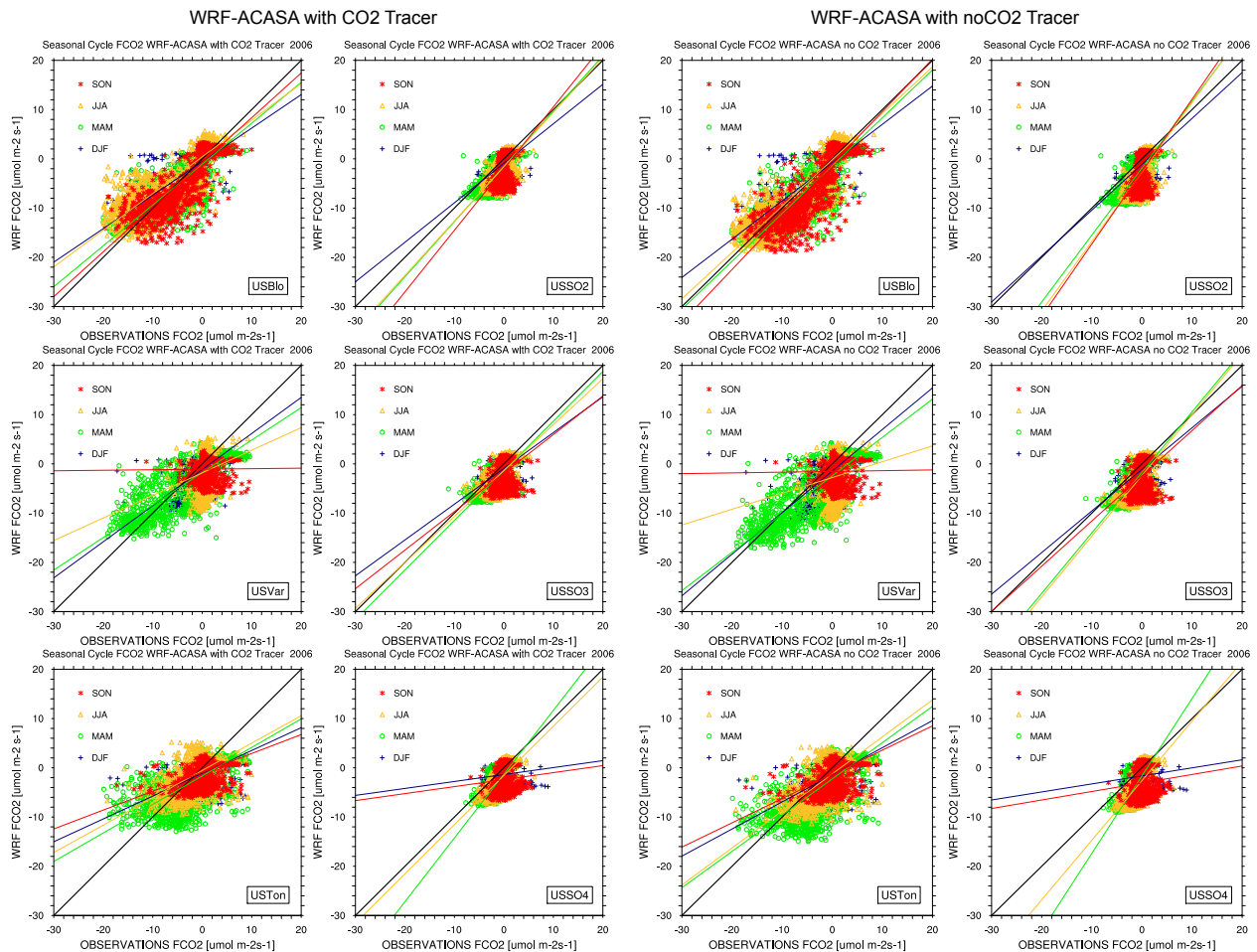


**Figure 4.** Scatter plots of CO<sub>2</sub> flux (FCO<sub>2</sub>) by season for both WRF-ACASA with CO<sub>2</sub> tracer and WRF-ACASA without CO<sub>2</sub> tracer. Each dot represent one daily value, and each line represent the regression of the season. Winter is in blue (DJF), Spring is green (MAM). Summer is orange (JJA). And fall is red (SON).

the observed annual NEE of  $-505 \text{ gC m}^{-2} \text{ yr}^{-1}$ .

There is, however, a large interannual variability between 2005 and 2006. Carbon sinks were larger for most sites in 2005, except the Blodgett Forest. The WRF-ACASA with CO<sub>2</sub> tracer underestimated the annual NEE magnitude in 2006 for the Blodgett Forest mainly due to the underestimation of photosynthesis during the summer months as indicated in Fig. 2 and Fig. 3. Meanwhile, the model overestimated the carbon uptake for the Tonzi Ranch during the autumn season for 2006. The carbon sinks for Vaira Ranch, Tonzi Ranch and the three Sky Oaks sites are also smaller in 2006 than 2005. Although the WRF-ACASA model overestimated the NEE for the Sky Oak sites due to the initial mismatch of PFT, improvement in PFT will improve the WRF-ACASA model by using more appropriate parameters such as maximum carboxylation velocity for physiological processes.

The spatial distributions of NEE for the four seasons using the WRF-ACASA model with and without CO<sub>2</sub> tracer are shown in Fig. 7. The inclusion of CO<sub>2</sub> tracer in the model reduced the

**Table 2.** Statistical Analysis for WRF-ACASA with no CO<sub>2</sub> tracer and with CO<sub>2</sub> tracer.

Station	DJF		MAM		JJA		SON	
	RMSE	R <sup>2</sup>	RMSE	R <sup>2</sup>	RMSE	R <sup>2</sup>	RMSE	R <sup>2</sup>
<b>WRF-ACASA no CO<sub>2</sub> Tracer</b>								
USBlo	2.79	0.89	3.44	0.95	3.58	0.99	3.66	0.96
USVar	3.00	0.76	4.51	0.82	5.14	0.16	3.84	0.06
USTon	3.61	0.37	4.98	0.69	3.67	0.62	3.35	0.30
USSO2	1.93	0.79	3.25	0.77	4.04	0.72	4.11	0.71
USSO3	1.89	0.76	3.01	0.80	3.71	0.76	3.89	0.71
USSO4	2.78	0.26	3.21	0.75	3.84	0.73	4.52	0.28
<b>WRF-ACASA with CO<sub>2</sub> Trace</b>								
USBlo	2.67	0.80	3.08	0.94	4.32	0.82	3.16	0.97
USVar	2.71	0.68	4.28	0.71	3.99	0.23	3.30	0.05
USTon	3.26	0.31	4.83	0.48	3.45	0.35	3.02	0.19
USSO2	1.65	0.77	2.54	0.82	2.75	0.81	3.29	0.74
USSO3	1.63	0.72	2.35	0.84	2.51	0.83	3.14	0.69
USSO4	2.49	0.24	2.42	0.80	2.54	0.79	3.70	0.25

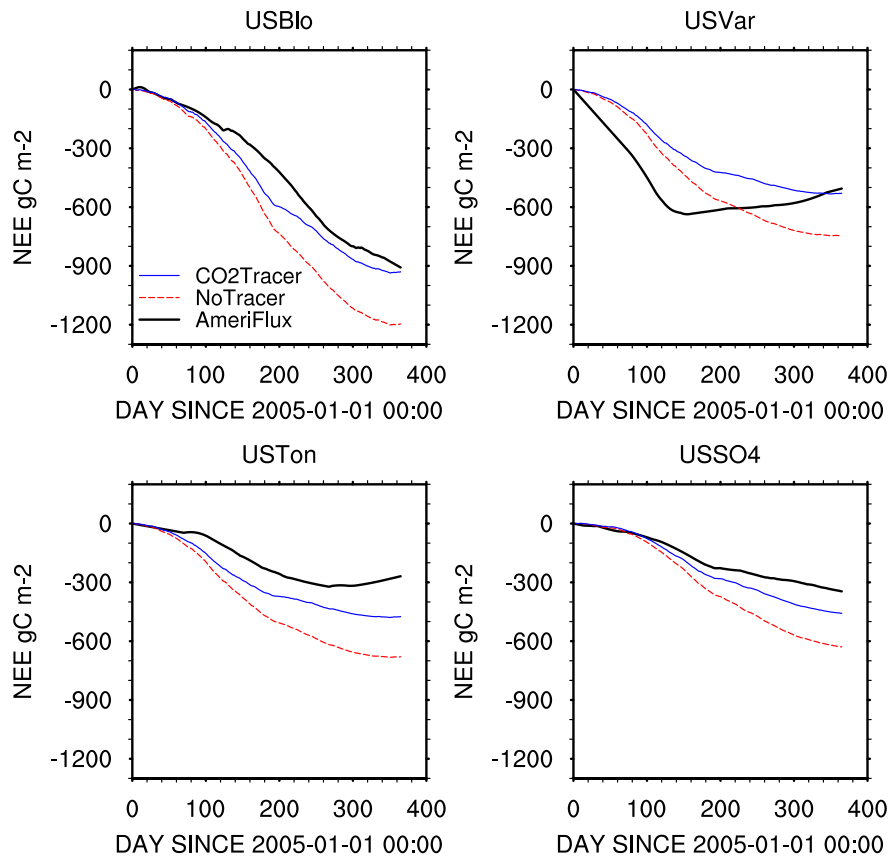


**Figure 5.** Time series of annual NEE for model simulations and surface observations for year 2005. The black line is observation, the red line is WRF-ACASA result without CO<sub>2</sub> tracer, and the blue line is WRF-ACASA result with CO<sub>2</sub> tracer.

seasonal NEE in several regions in California. The differences between the two simulations are small during the winter and autumn seasons, which are similar to the results shown in Figure 2;

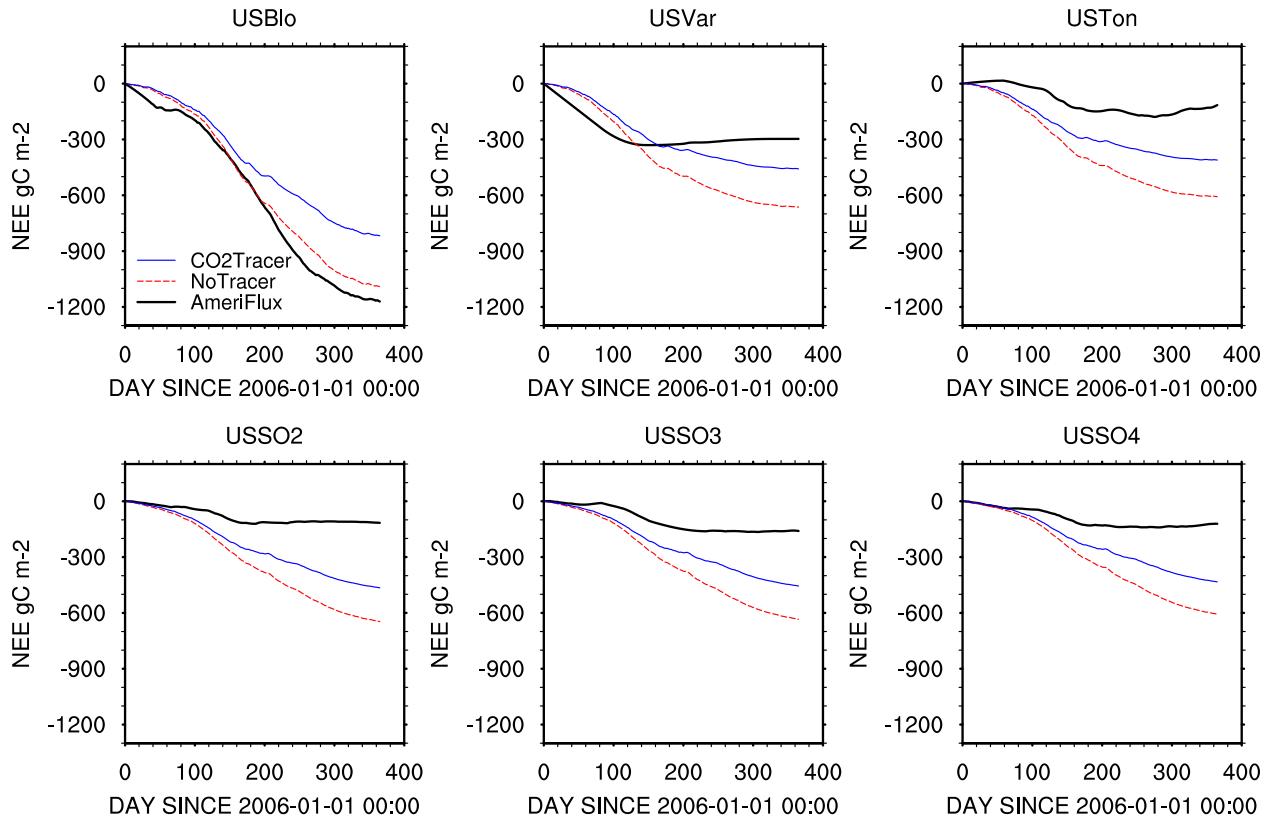


**Figure 6.** Time series of annual NEE for model simulations and surface observations for year 2006. The black line is observation, the red line is WRF-ACASA result without CO<sub>2</sub> tracer, and the blue line is WRF-ACASA result with CO<sub>2</sub> tracer.

not surprisingly since the NEE magnitudes are smaller, and therefore the effects of advected CO<sub>2</sub> are reduced. During spring and summer, when plants are more active, the seasonal carbon sink or negative NEE values over the Sierra Nevada mountain region is smaller when CO<sub>2</sub> tracer is used. Furthermore, the Central Valley changed from a carbon sink when no CO<sub>2</sub> tracer is used to a carbon source with CO<sub>2</sub> tracer during the summer months. This is due to the reduction in photosynthesis in response to the lower ambient CO<sub>2</sub> concentration when carbon (or in this case, depleted carbon concentrations) is transported in the atmosphere. This switch of carbon sink to carbon source demonstrates the importance of a fully coupled biosphere-atmosphere interaction. Feedbacks between the two systems through exchange and transport of carbon reflect a more realistic representation of the natural processes of interaction between ecosystems and the atmosphere, and with advection of carbon dioxide concentrations, between the atmosphere and ecosystems downwind.

Overall, the annual NEE for 2006 show that plants in the Northern California regions actively uptake more carbon dioxide from the atmosphere than carbon emissions through respiration, creating net carbon sinks (Fig. 8). The Southern California regions, which include the Mojave Desert and other low-vegetation regions, are carbon sources, where more carbon is released into the atmosphere than is absorbed. The coupled CO<sub>2</sub> tracer reduced the annual NEE over the northern California and the Sierra Nevada mountain regions. The regions with large carbon sources as

**Table 3.** Annual NEE ( $\text{gC m}^{-2} \text{yr}^{-1}$ ) of the six AmeriFlux sites for years 2005 and 2006. Due to large amount of missing data in 2005, no data is displayed for Sky Oak sites: USSO2 and USSO3.

Year	Site	OBS	WRF-ACASA without CO <sub>2</sub> tracer	WRF-ACASA with CO <sub>2</sub> tracer
2005	USBlo	-908	-1197	-930
	USVar	-506	-744	-529
	USTon	-269	-679	-475
	USSO2	No Data	-670	-491
	USSO3	No Data	-658	-481
	USSO4	-346	-629	-458
	2006	USBlo	-1171	-1091
USVar		-297	-664	-458
USTon		-116	-608	-411
USSO2		-116	-647	-465
USSO3		-160	-635	-456
USSO4		-121	-607	-433

indicated in red are generally urban areas where more carbon dioxide is released into the atmosphere than carbon uptake by vegetation. Default urban carbon emission from traffic is based on urban land use area. Future improvement on urban emission will link the model to observed urban population and traffic data. Even though, the WRF-ACASA model overestimated carbon uptakes for the AmeriFlux sites due to various reasons mentioned previously, the CO<sub>2</sub> concentration and transport in the atmosphere have an important role in modeling plant physiological processes.

Diurnal patterns of ambient CO<sub>2</sub> concentration are compared for each AmeriFlux site between observed values and the simulated values by the WRF-ACASA model, in which CO<sub>2</sub> tracer is used to transport carbon dioxide in the atmosphere (Fig. 9 and Fig. 10). They show that the CO<sub>2</sub> tracer in the WRF-ACASA model is able to mimic the natural evolution of atmospheric CO<sub>2</sub> concentration (ACO<sub>2</sub>) due to changes in surface plant physiological processes and atmospheric transport. Photosynthesis from the vegetation actively removes carbon dioxide from the atmosphere and thus lowers the ambient CO<sub>2</sub> concentration during the daytime, whereas respiration increases the ambient CO<sub>2</sub> concentration.

When PFTs match between site observations and model assumptions, the simulated concentrations over the Blodgett Forest and the Tonzi Ranch have good agreements with the surface observation. The reduction of ambient CO<sub>2</sub> concentration is more pronounced over sites with higher plant physiological activities such as the Blodgett Forest, the Vaira and Tonzi ranches. For both years, the Blodgett Forest reduced the ambient CO<sub>2</sub> concentration by an average of 6 to 7 ppm during the daytime. The lower ambient CO<sub>2</sub> concentration persisted into the evening, when respiration slowly increased the CO<sub>2</sub> concentration toward and exceeded the initial 385 ppm. The time lags in the diurnal patterns of atmospheric CO<sub>2</sub> concentration compared to the diurnal patterns of CO<sub>2</sub> flux reflect the cumulative effect of daytime and nighttime carbon dioxide exchanges between the biosphere and atmosphere. Meanwhile, the atmospheric CO<sub>2</sub> concentration over the Sky Oaks sites exceeded the initial concentration during the winter season when plants released more CO<sub>2</sub> into the atmosphere than uptake by photosynthesis.



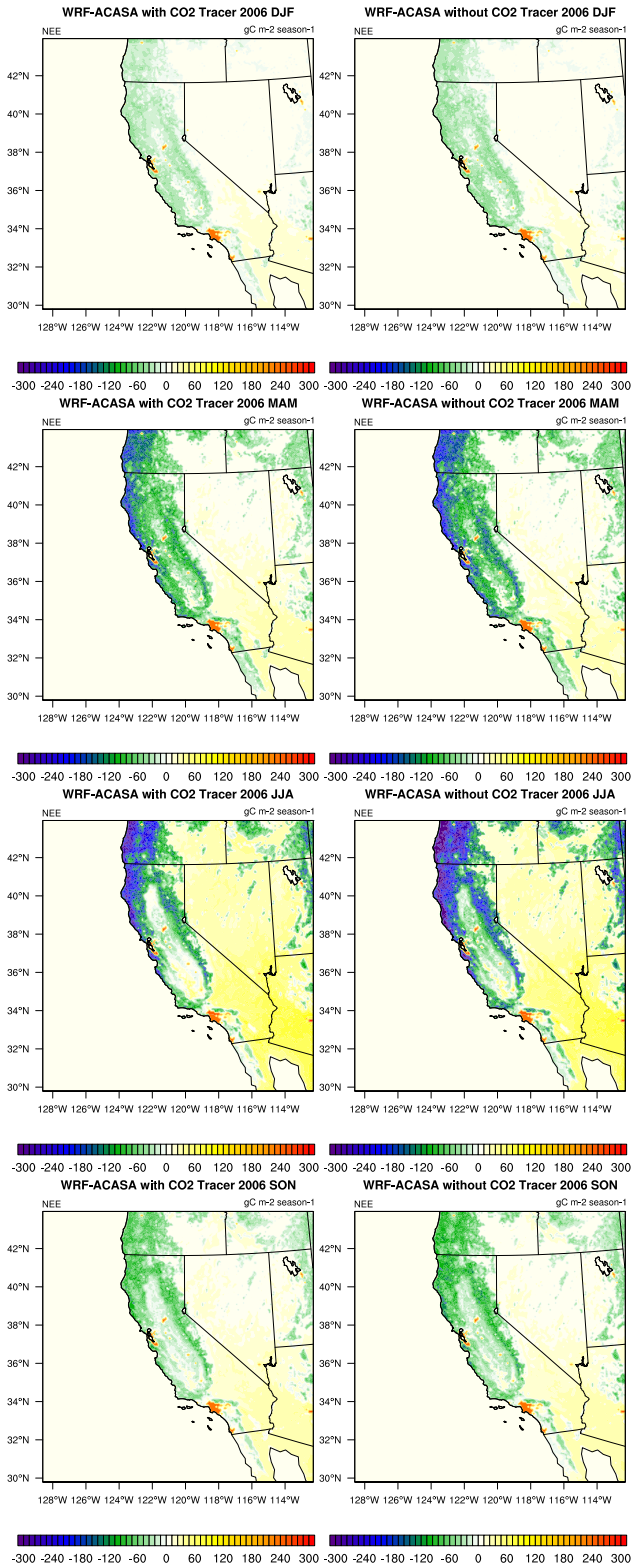


**Figure 7.** WRF-ACASA simulations of seasonal NEE with and without CO<sub>2</sub> Tracer for 2006. Winter is DJF. Spring is MAM. Summer is JJA. And fall is SON. Results for 2005 (not shown) is similar to 2006.

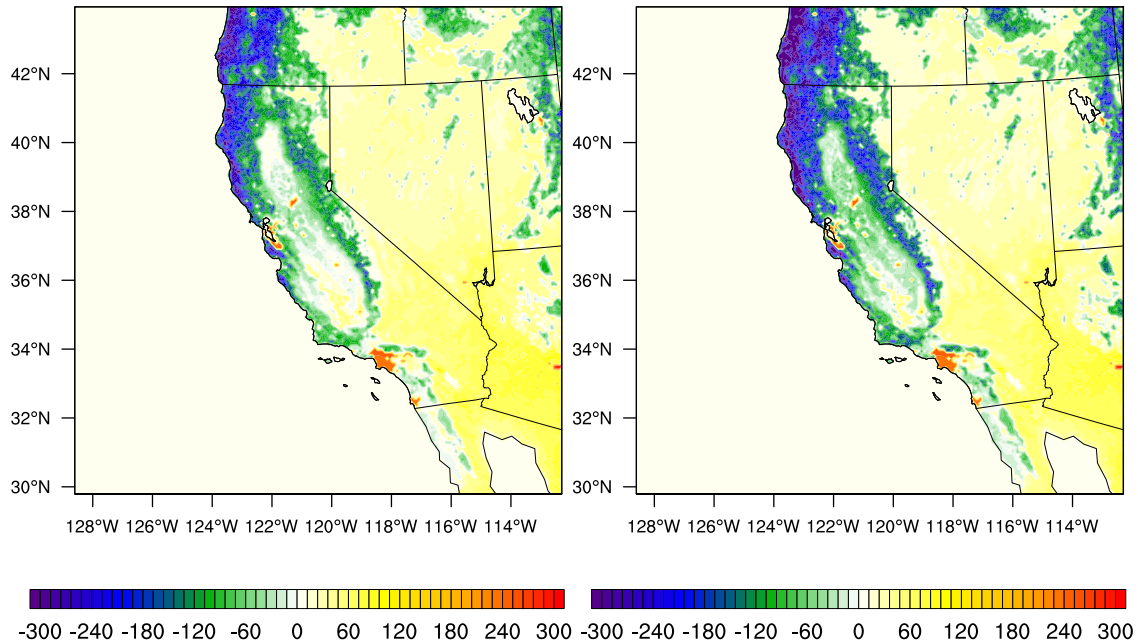


**Figure 8.** Annual NEE of carbon dioxide for year 2006 for WRF-ACASA simulations with CO<sub>2</sub> tracer (Left) and without CO<sub>2</sub> tracer (Right).

Over the Sky Oak sites where mismatch of PFT occurs, there are large differences between the simulated and observed diurnal pattern of ACO<sub>2</sub>. The poor performance over the Sky Oak sites could be the result of initial conditions at the sites, where the constant field of 385 ppm applied over the domain is much higher than the observed ACO<sub>2</sub> (around 365 to 370 ppm). Despite the bias from initial conditions, the changes in time and magnitude from the simulated ACO<sub>2</sub> match well with the observed ACO<sub>2</sub> seasonal and diurnal patterns for both year 2005 and 2006. While there are no data to evaluate the model performance in atmospheric carbon dioxide concentration over the entire region, the evaluations from the AmeriFlux sites shows that the CO<sub>2</sub> tracer in the WRF-ACASA model is robust and physically sound.

The WRF-ACASA model with CO<sub>2</sub> tracer simulates the seasonal averages of ACO<sub>2</sub> at different vertical levels. The spatial distribution of ACO<sub>2</sub> anomalies from the initial field of 385 ppm is shown in Fig. 11 for the year 2006, because the CO<sub>2</sub> is transported both horizontally and vertically. Surface CO<sub>2</sub> concentration (sigma level 1) closely follows the plant physiological processes as shown in Fig. 7 and Fig. 8. The spatial distributions of ACO<sub>2</sub> at higher vertical levels, however, show that the CO<sub>2</sub> concentration above the surface is also modified by transport of CO<sub>2</sub> through wind and diffusion. For example, during the summer of 2006 the large reduction of ACO<sub>2</sub> at the surface (sigma level 1) from photosynthesis propagated into the upper levels (sigma levels 3, 7 and 10) and spread to the surrounding areas. At sigma level 13, the surface effect on ACO<sub>2</sub> became negligible compared to the lower levels. As the vertical level increases, the effects on surface CO<sub>2</sub> flux decrease, and the CO<sub>2</sub> transport increases spatially to reach farther regions. Therefore, surface plant activities from one location would have an impact on the neighboring

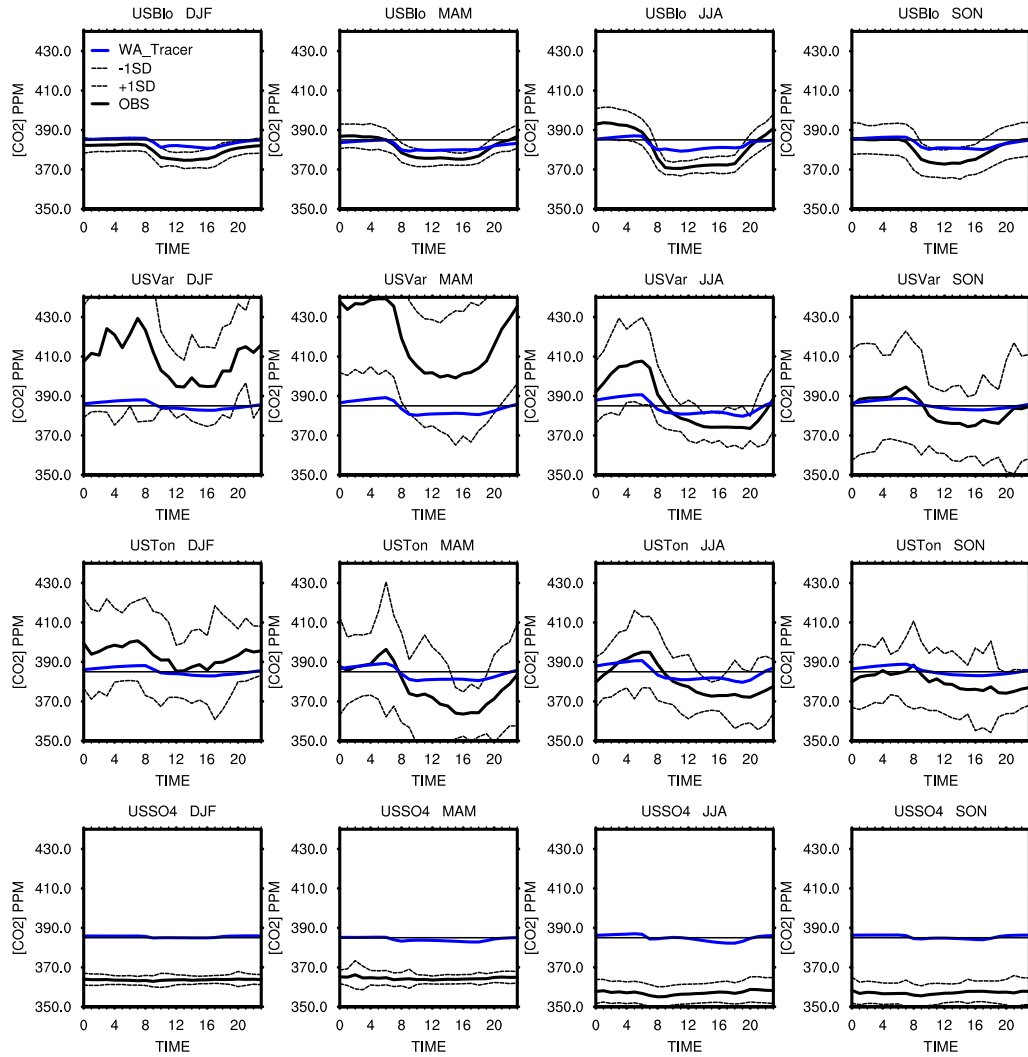


**Figure 9.** Seasonal diurnal patterns of atmosphere carbon dioxide concentration for the six AmeriFlux sites for year 2005. Black solid lines represent observation from AmeriFlux sites, and black dash lines represent one standard deviation below and above the diurnal means. Blue lines are WRF-ACASA simulations with CO<sub>2</sub> tracer. Winter is DJF. Spring is MAM. Summer is JJA. And fall is SON.

ecosystems as CO<sub>2</sub> concentration is transported in the atmosphere both spatially and temporally.

Furthermore, Fig. 12 shows the effect of plant physiological processes from one location on the neighboring ecosystems. The time series graphs of ACO<sub>2</sub> show that the CO<sub>2</sub> tracer transports the enhanced atmospheric CO<sub>2</sub> concentration from Los Angeles due to morning traffic eastward to the neighboring ecosystems. This CO<sub>2</sub> enrichment therefore influences the plant physiological processes in nearby regions. Active photosynthesis in the Northern California, on the other hand, creates lower ACO<sub>2</sub> air parcels that move southward to offset the urban carbon emission from San Francisco Bay and Sacramento regions.

The illustration of the vertical and horizontal transport of ACO<sub>2</sub> is also displayed in the vertical cross-section of a ACO<sub>2</sub> transect that stretches from the central coast across the Central Valley and to the Sierra Nevada Mountains (Fig. 13). The impact of surface plant physiological

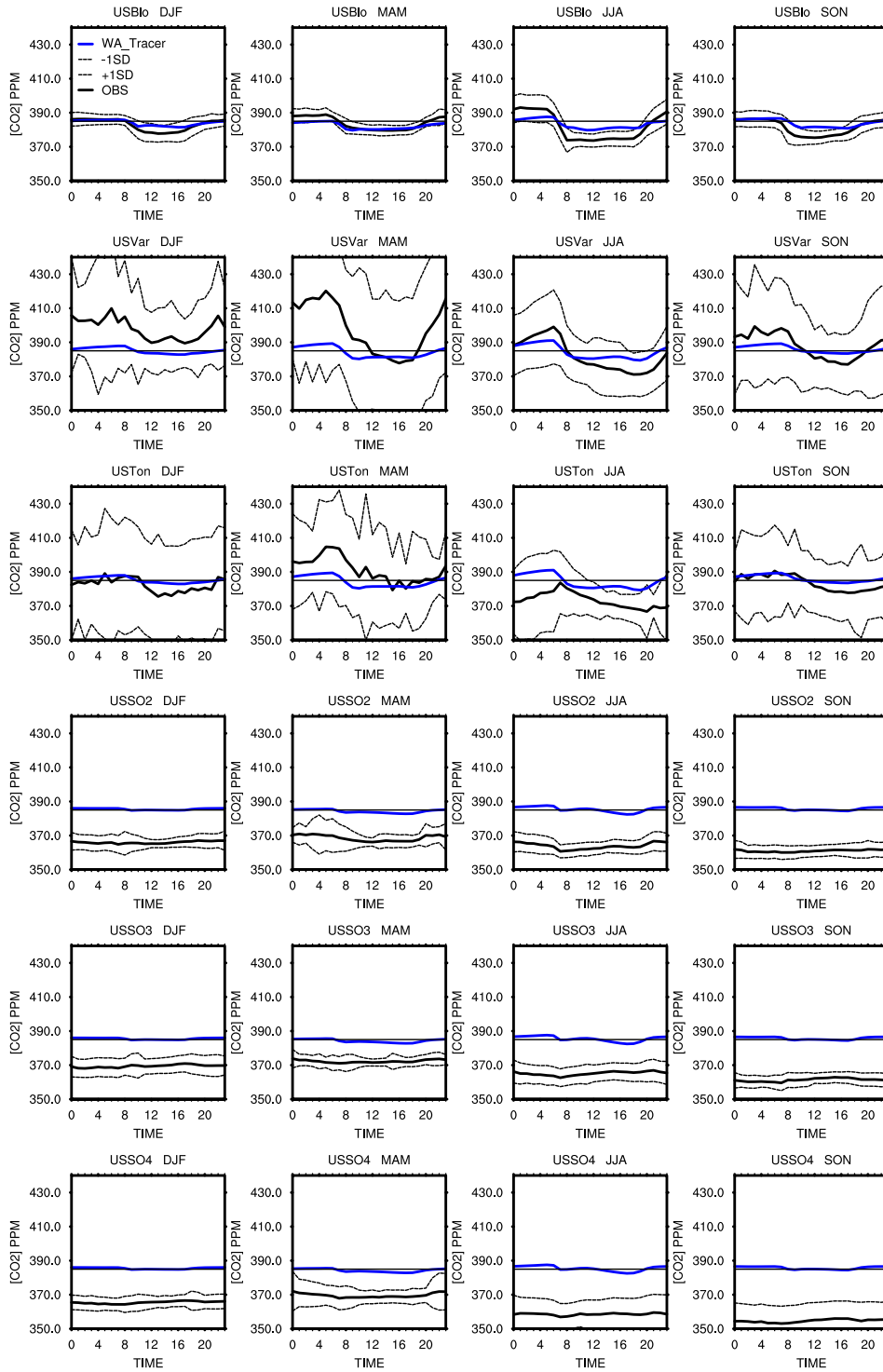


**Figure 10.** Seasonal diurnal patterns of atmosphere carbon dioxide concentration for the six AmeriFlux sites for year 2006. Black solid lines represent observation from AmeriFlux sites, and black dash lines represent one standard deviation below and above the diurnal means. Blue lines are WRF-ACASA simulations with CO<sub>2</sub> tracer.

processes that change the atmospheric CO<sub>2</sub> concentration propagates high into the atmosphere and spreads throughout the region. During the nighttime, respiration increases the ACO<sub>2</sub> near the

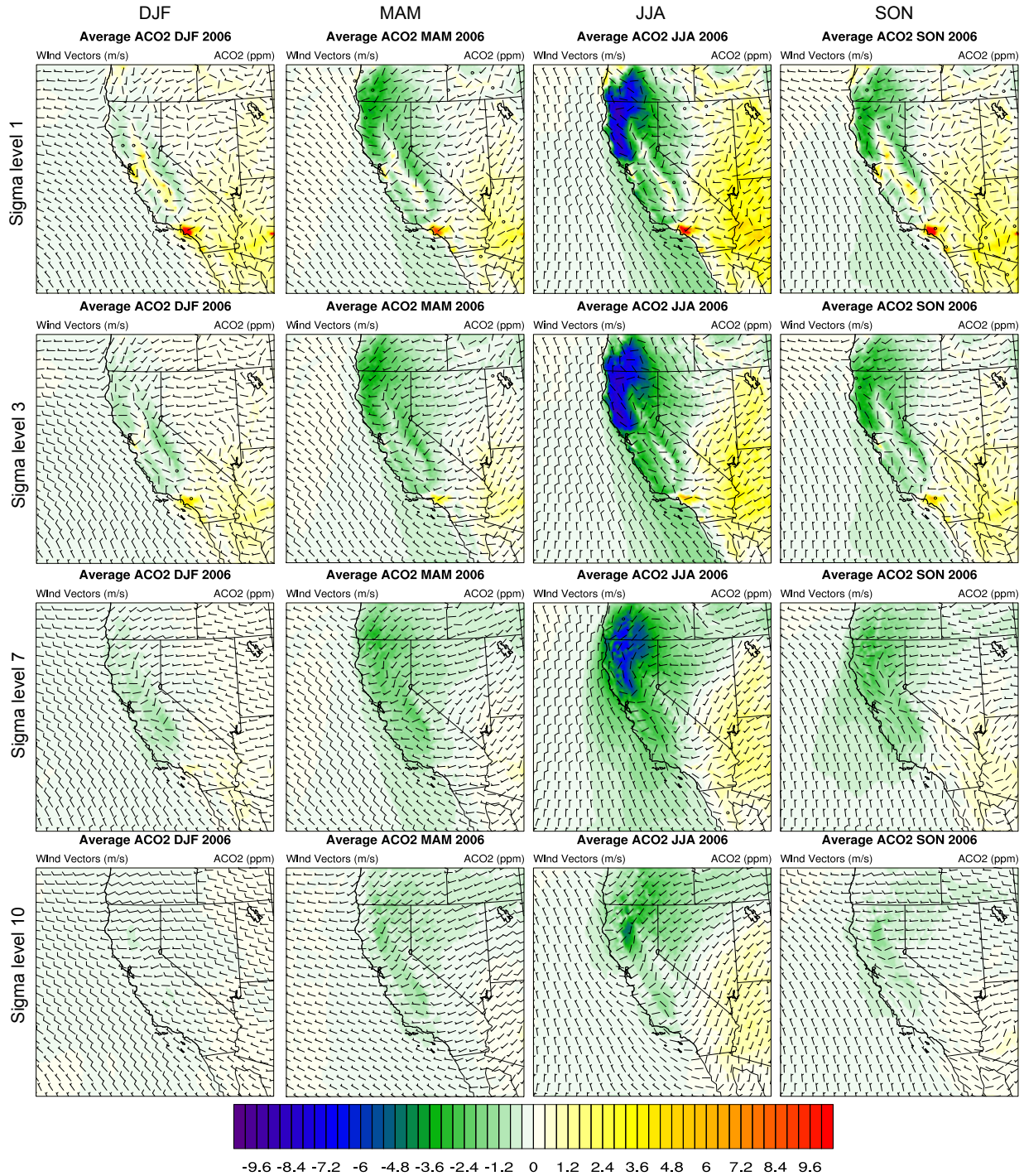


**Figure 11.** Map of atmospheric CO<sub>2</sub> concentrations and wind patterns using the CO<sub>2</sub> tracer by seasons and sigma levels for year 2006.

surface and increases ACO<sub>2</sub> over the Central Valley. The marine layer wind patterns carry these higher atmospheric CO<sub>2</sub> concentrations eastward toward the foothills and up the Sierra Nevada Mountains. Photosynthesis during the daytime reduces the surface ACO<sub>2</sub>. Stable atmospheric conditions allow the lower ACO<sub>2</sub> parcels to extend upward as shown during midday of Fig. 13.

Land and sea breezes transport plumes of higher or lower CO<sub>2</sub> concentration air parcels across the region and influence the local ecosystems. Figure 13 demonstrates the interactions of neighboring ecosystems through atmospheric CO<sub>2</sub> transport at a regional scale. Plant physiological processes from one location would have an impact on the neighboring ecosystems.

#### 4. SUMMARY AND CONCLUSION

In this study, a coupled WRF-ACASA model was used with a new CO<sub>2</sub> tracer routine to simulate CO<sub>2</sub> exchange between the atmosphere and the biosphere as well as the effect of CO<sub>2</sub> transport on surface plant physiology. Two simulations of CO<sub>2</sub> fluxes and ACO<sub>2</sub> using the WRF-ACASA model with and without CO<sub>2</sub> tracers were performed over California for the years 2005 and 2006. The ACASA surface scheme calculated physiological processes of photosynthesis and respiration at the local surface level and carbon fluxes were fed back into the WRF atmosphere layers above. The CO<sub>2</sub> tracer modified the atmospheric CO<sub>2</sub> concentration according to the surface carbon fluxes and transported carbon dioxide both spatially and temporally through wind and diffusion. This two-way feedback between the biosphere and atmosphere reflected a more realistic representation of the natural system. Communications through carbon dioxide exchange between the various ecosystems allow us to examine the interactions across different geographical regions and identify the possible sources and sinks of carbon. Seasonal and annual distribution of carbon sinks and sources were determined.

When the model PFTs match the observed PFTs, carbon dioxide fluxes from the WRF-ACASA simulations agree well with the surface observations. For example, the simulated diurnal patterns of CO<sub>2</sub> flux for the Blodgett Forest match well with the surface observations. Although the WRF-ACASA model overestimates the three Sky Oak sites and Vaira Ranch, the biases are due to initial PFT mismatch and lack of homogeneous land cover type in the grid cell rather than the model physics. As pointed out in the previous chapters, surface representation is crucial to the

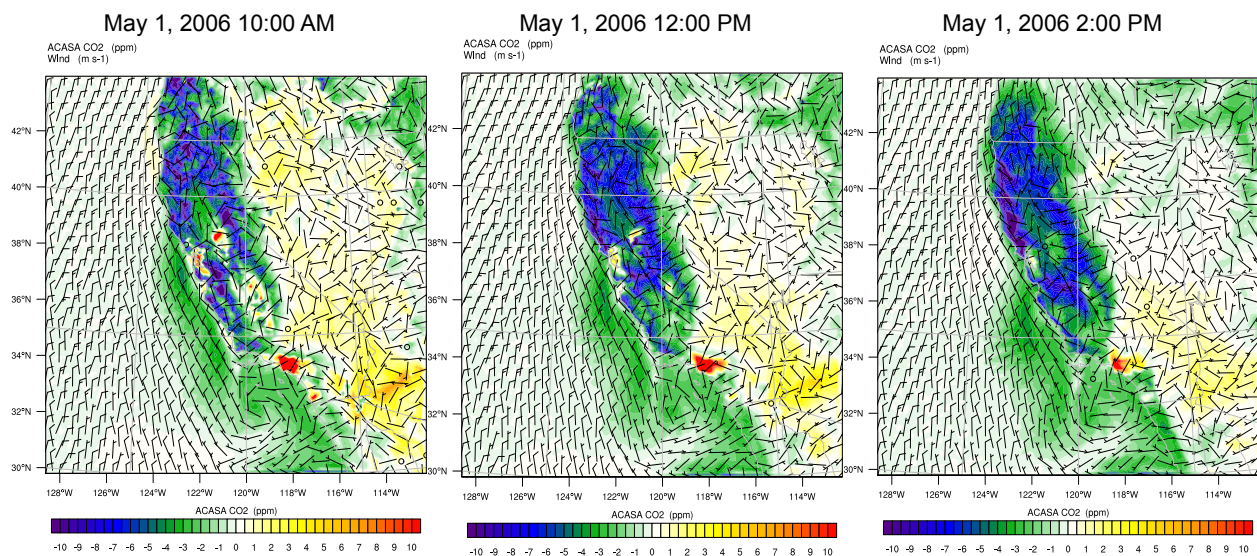


**Figure 12.** Atmospheric CO<sub>2</sub> concentration of May 1 2006 for 10 AM, 12 PM, and 2 PM.

high complexity WRF-ACASA model. Improvement of PFT as well as inclusion of more than one vegetation type in each of the grid cell will improve the WRF-ACASA model performance for CO<sub>2</sub> flux.

There is a positive impact on simulating plant physiological processes from varying atmospheric CO<sub>2</sub> concentrations. The inclusion of the CO<sub>2</sub> tracer in the WRF-ACASA model reduces the overestimate of photosynthesis for most of the AmeriFlux sites. Active CO<sub>2</sub> uptake by plants reduces the ambient CO<sub>2</sub> concentration and thus lowers available CO<sub>2</sub> for plant physiological ac-

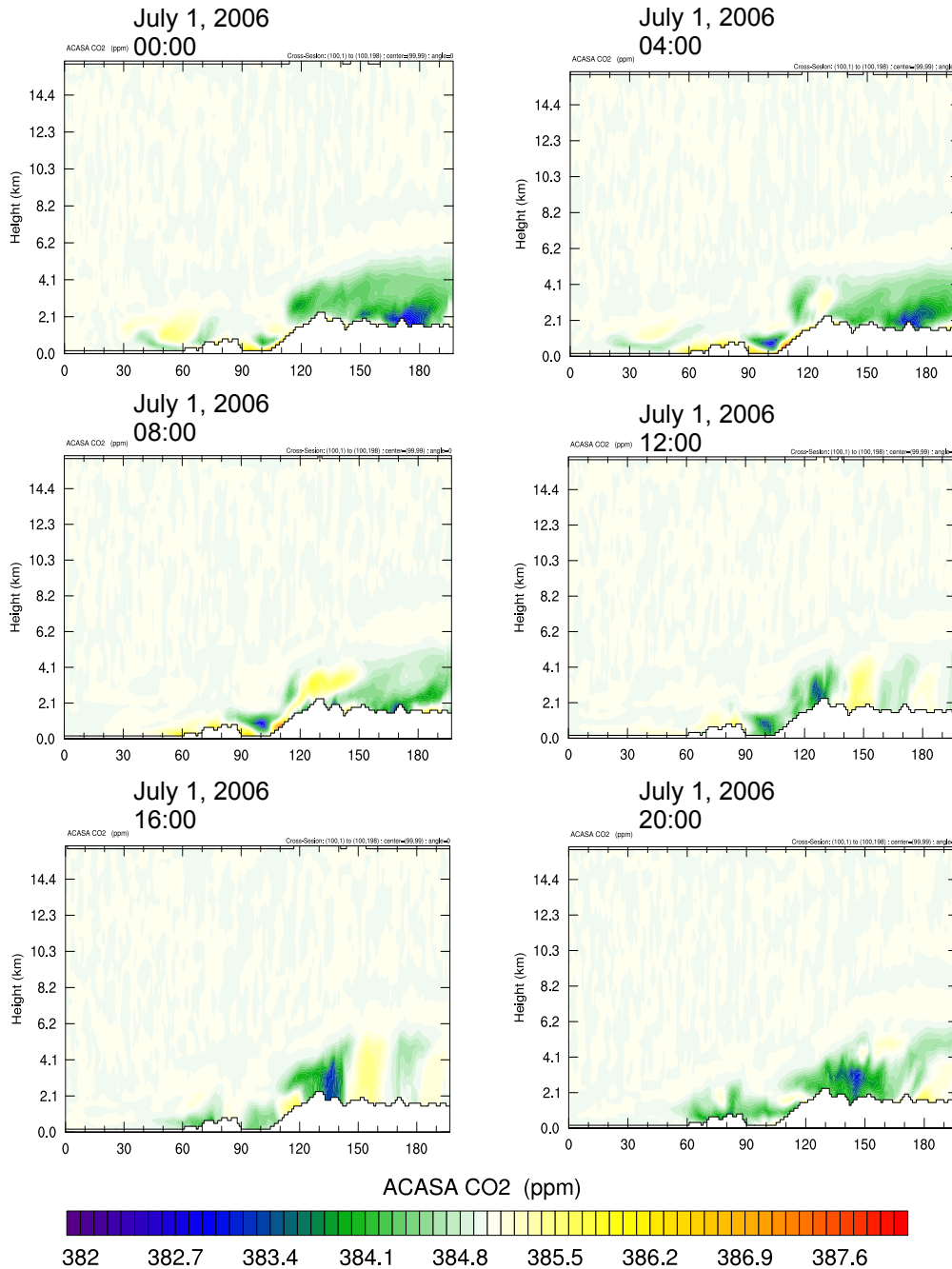


**Figure 13.** Vertical Cross-section of atmospheric CO<sub>2</sub> concentration.

tivities during the daytime. The CO<sub>2</sub> tracer therefore helps reduce the RMSE values for hourly CO<sub>2</sub> fluxes as well as improve the annual NEE. In addition, the effect of CO<sub>2</sub> transport in the atmosphere is not limited to the local areas as CO<sub>2</sub> is transported both horizontally and vertically throughout the region. Atmospheric transport of CO<sub>2</sub> concentration allows surface activities from one region to influence the neighboring ecosystems.

Overall, this study shows that the WRF-ACASA model is robust and able to simulate the CO<sub>2</sub> fluxes well across the region if given correct surface representations. The comparison between the two model simulations with and without the CO<sub>2</sub> tracer shows that the impact of atmospheric CO<sub>2</sub> transport is important and it should not be neglected when simulating CO<sub>2</sub> flux at a regional scale. The interactions between atmosphere and biosphere as well as between neighboring ecosystems influence the plant physiological processes at both local and regional levels.

It must be noted that the atmospheric CO<sub>2</sub> concentration in this study is initialized with a constant field of 385 ppm, and it changes through time and space from surface processes. This initial condition, however, might not reflect the actual atmospheric concentrations since there are no available observations. Therefore, spatially distributed measurements of atmospheric CO<sub>2</sub> concentration could be a valuable input for the WRF-ACASA model in the future.

## Acknowledgements

This work is supported in part by the National Science Foundation under Awards No.ATM-0619139 and EF-1137306. The Joint Program on the Science and Policy of Global Change is funded by a number of federal agencies and a consortium of 40 industrial and foundation sponsors. (For the complete list see <http://globalchange.mit.edu/sponsors/current.html>).

## 5. REFERENCES

- Anthes, R., 1984: Enhancement of convective precipitation by mesoscale variations in vegetative covering in semiarid regions. *J. Climate Appl. Meteor.*, **23**(4): 541–554.
- Baldocchi, D. and T. Meyers, 1998: On using eco-physiological, micrometeorological and biogeochemical theory to evaluate carbon dioxide, water vapor and trace gas fluxes over vegetation: a perspective. *Agric. For. Meteor.*, **90**(1-2): 1–25.
- Baldocchi, D., E. Falge, L. Gu, R. Olson, D. Hollinger, S. Running, P. Anthoni, C. Bernhofer, K. Davis, R. Evans *et al.*, 2001: FLUXNET: a new tool to study the temporal and spatial variability of ecosystem-scale carbon dioxide, water vapor, and energy flux densities. *Bull. Amer. Meteor. Soc.*, **82**(11): 2415–2434.
- Bougeault, P., 1991: Parameterization schemes of land-surface processes for mesoscale atmospheric models. *Land Surface Evaporation: Measurements and Parameterization*, pp. 55–92.
- Chen, S. and W. Sun, 2002: A one-dimensional time dependent cloud model. *J. Meteor. Soc. Japan*, **80**(1): 99–118.
- Collatz, G., J. Ball, C. Grivet and J. Berry, 1991: Physiological and environmental regulation of stomatal conductance, photosynthesis and transpiration: a model that includes a laminar boundary layer. *Agric. For. Meteor.*, **54**(2): 107–136.



- Collins, W., V. Ramaswamy, M. Schwarzkopf, Y. Sun, R. Portmann, Q. Fu, S. Casanova, J. Dufresne, D. Fillmore, P. Forster *et al.*, 2006: Radiative forcing by well-mixed greenhouse gases: Estimates from climate models in the Intergovernmental Panel on Climate Change (IPCC) Fourth Assessment Report (AR4). *J. Geophys. Res.*, **111**(D14): D14317.
- Dudhia, J., 1989: Numerical study of convection observed during the winter monsoon experiment using a mesoscale two-dimensional model. *J. Atmos. Sci.*, **46**(20): 3077–3107.
- Falge, E., D. Baldocchi, J. Tenhunen, M. Aubinet, P. Bakwin, P. Berbigier, C. Bernhofer, G. Burba, R. Clement, K. Davis *et al.*, 2002: Seasonality of ecosystem respiration and gross primary production as derived from FLUXNET measurements. *Agric. For. Meteorol.*, **113**(1): 53–74.
- Farquhar, G., S. Von Caemmerer *et al.*, 1982: Modelling of photosynthetic response to environmental conditions. *Encyclopedia of plant physiology*, **12**: 549–587.
- Hong, S. and H. Pan, 1996: Nonlocal boundary layer vertical diffusion in a medium-range forecast model. *Mon. Wea. Rev.*, **124**(10): 2322–2339.
- Klemp, J., W. Skamarock and O. Fuhrer, 2003: Numerical consistency of metric terms in terrain-following coordinates. *Mon. Wea. Rev.*, **131**(7): 1229–1239.
- Laprise, R., 1992: The Euler equations of motion with hydrostatic pressure as an independent variable. *Mon. Wea. Rev.*, **120**(1): 197–207.
- Law, B., 2007: AmeriFlux network aids global synthesis. *Eos*, **88**(28): 286.
- Leuning, R., 1990: Modelling stomatal behaviour and photosynthesis of eucalyptus grandis. *Aust. J. Plant Physiol.*, **17**(2): 159–175.
- Marras, S., R. Pyles, C. Sirca, K. Paw U, R. Snyder, P. Duce and D. Spano, 2011: Evaluation of the Advanced Canopy–Atmosphere–Soil Algorithm (ACASA) model performance over Mediterranean maquis ecosystem. *Agric. For. Meteorol.*, **151**(6): 730–745.
- Mesinger, F., G. DiMego, E. Kalnay, K. Mitchell, P. Shafran, W. Ebisuzaki, D. Jovic, J. Woollen, E. Rogers, E. Berbery *et al.*, 2006: North American regional reanalysis. *Bull. Amer. Meteor. Soc.*, **87**(3): 343–360.
- Meyers, T. and K. Paw U, 1986: Testing of a Higher-Order Closure Model for Modeling Airflow within and above Plant Canopies. *Bound.Lay. Meteorol.*, **37**: 297–311.
- Meyers, T. and K. Paw U, 1987: Modelling the plant canopy micrometeorology with higher-order closure principles. *Agric. For. Meteorol.*, **41**(1): 143–163.
- Mihailovic, D., R. Pielke, B. Rajkovic, T. Lee and M. Jeftic, 1993: A resistance representation of schemes for evaporation from bare and partly plant-covered surfaces for use in atmospheric models. *J. Appl. Meteorol.*, **32**: 1038–1054.

- Mlawer, E., S. Taubman, P. Brown, M. Iacono and S. Clough, 1997: Radiative transfer for inhomogeneous atmospheres: RRTM, a validated correlated-k model for the longwave. *J. Geophys. Res.*, **102**(D14): 16663–16.
- Monin, A. and A. Obukhov, 1954: Basic laws of turbulent mixing in the atmosphere near the ground. *Tr. Akad. Nauk SSSR Geofiz. Inst.*, **24**(151): 163–87.
- Paw U, K., 1997: The Modeling and Analysis of Crop Canopy Interactions with the Atmosphere under Global Climatic Change Conditions. *J. Agric. Meteorol.*, **52**(5): 419–428.
- Paw U, K. and W. Gao, 1988: Applications of solutions to non-linear energy budget equations. *Agric. For. Meteorol.*, **43**(2): 121–145.
- Paw U, K., M. Falk, T. Suchanek, S. Ustin, J. Chen, Y. Park, W. Winner, S. Thomas, T. Hsiao, R. Shaw *et al.*, 2004: Carbon dioxide exchange between an old-growth forest and the atmosphere. *Ecosystems*, **7**(5): 513–524.
- Potter, C., J. Randerson, C. Field, P. Matson, P. Vitousek, H. Mooney and S. Klooster, 1993: Terrestrial ecosystem production: a process model based on global satellite and surface data. *Global Biogeochem. Cycles*, **7**(4): 811–841.
- Pyles, R., 2000: *The development and testing of the UCD Advanced Canopy–Atmosphere–Soil Algorithm (ACASA) for use in climate prediction and field studies*. Ph.D. Thesis, University of California, Davis.
- Pyles, R., B. Weare and K. Paw U, 2000: The UCD Advanced Canopy-Atmosphere-Soil Algorithm: comparisons with observations from different climate and vegetation regimes. *Quart. J. Roy. Meteor. Soc.*, **126**: 2951–2980.
- Sagan, C. and B. Khare, 1979: Tholins-organic chemistry of interstellar grains and gas. *Nature*, **277**: 102–107.
- Staudt, K., E. Falge, R. Pyles and T. FOKEN, 2010: Sensitivity and predictive uncertainty of the ACASA model at a spruce forest site. *Biogeosciences*, **7**(11): 3685–3705.
- Wigley, T. and D. Schimel, 2005: *The carbon cycle*, volume 6. Cambridge University Press.
- Wohlfahrt, G., M. Bahn, U. Tappeiner and A. Cernusca, 2001: A multi-component, multi-species model of vegetation–atmosphere CO<sub>2</sub> and energy exchange for mountain grasslands. *Agric. For. Meteorol.*, **106**(4): 261–287.

## REPORT SERIES of the MIT Joint Program on the Science and Policy of Global Change

FOR THE COMPLETE LIST OF JOINT PROGRAM REPORTS: <http://globalchange.mit.edu/pubs/all-reports.php>

260. **Electricity Generation and Emissions Reduction Decisions under Policy Uncertainty: A General Equilibrium Analysis.** *Morris et al.*, April 2014
261. **An Integrated Assessment of China's Wind Energy Potential.** *Zhang et al.*, April 2014
262. **The China-in-Global Energy Model.** *Qi et al.* May 2014
263. **Markets versus Regulation: The Efficiency and Distributional Impacts of U.S. Climate Policy Proposals.** *Rausch and Karplus*, May 2014
264. **Expectations for a New Climate Agreement.** *Jacoby and Chen*, August 2014
265. **Coupling the High Complexity Land Surface Model ACASA to the Mesoscale Model WRF.** *Xu et al.*, August 2014
266. **The CO<sub>2</sub> Content of Consumption Across US Regions: A Multi-Regional Input-Output (MRIO) Approach.** *Caron et al.*, August 2014
267. **Carbon emissions in China: How far can new efforts bend the curve?** *Zhang et al.*, October 2014
268. **Characterization of the Solar Power Resource in Europe and Assessing Benefits of Co-Location with Wind Power Installations.** *Bozonnat and Schlosser*, October 2014
269. **A Framework for Analysis of the Uncertainty of Socioeconomic Growth and Climate Change on the Risk of Water Stress: a Case Study in Asia.** *Fant et al.*, November 2014
270. **Interprovincial Migration and the Stringency of Energy Policy in China.** *Luo et al.*, November 2014
271. **International Trade in Natural Gas: Golden Age of LNG?** *Du and Paltsev*, November 2014
272. **Advanced Technologies in Energy-Economy Models for Climate Change Assessment.** *Morris et al.*, December 2014
273. **The Contribution of Biomass to Emissions Mitigation under a Global Climate Policy.** *Winchester and Reilly*, January 2015
274. **Modeling regional transportation demand in China and the impacts of a national carbon constraint.** *Kishimoto et al.*, January 2015
275. **The Impact of Advanced Biofuels on Aviation Emissions and Operations in the U.S.** *Winchester et al.*, February 2015
276. **Specifying Parameters in Computable General Equilibrium Models using Optimal Fingerprint Detection Methods.** *Koesler*, February 2015
277. **Renewables Intermittency: Operational Limits and Implications for Long-Term Energy System Models.** *Delarue and Morris*, March 2015
278. **The MIT EPPA6 Model: Economic Growth, Energy Use, and Food Consumption.** *Chen et al.*, March 2015
279. **Emulating maize yields from global gridded crop models using statistical estimates.** *Blanc and Sultan*, March 2015
280. **Water Body Temperature Model for Assessing Climate Change Impacts on Thermal Cooling.** *Strzepek et al.*, May 2015
281. **Impacts of CO<sub>2</sub> Mandates for New Cars in the European Union.** *Paltsev et al.*, May 2015
282. **Natural Gas Pricing Reform in China: Getting Closer to a Market System?** *Paltsev and Zhang*, July 2015
283. **Global population growth, technology, and Malthusian constraints: A quantitative growth theoretic perspective.** *Lanz et al.*, October 2015
284. **Capturing Natural Resource Dynamics in Top-Down Energy-Economic Equilibrium Models.** *Zhang et al.*, October 2015
285. **US Major Crops' Uncertain Climate Change Risks and Greenhouse Gas Mitigation Benefits.** *Sue Wing et al.*, October 2015
286. **Launching a New Climate Regime.** *Jacoby and Chen*, November 2015
287. **Impact of Canopy Representations on Regional Modeling of Evapotranspiration using the WRF-ACASA Coupled Model.** *Xu et al.*, December 2015
288. **The Influence of Gas-to-Liquids and Natural Gas Production Technology Penetration on the Crude Oil-Natural Gas Price Relationship.** *Ramberg et al.*, December 2015
289. **The Impact of Climate Policy on Carbon Capture and Storage Deployment in China.** *Zhang et al.*, December 2015
290. **Modeling Uncertainty in Climate Change: A Multi-Model Comparison.** *Gillingham et al.*, December 2015
291. **Scenarios of Global Change: Integrated Assessment of Climate Impacts.** *Paltsev et al.*, February 2016
292. **Costs of Climate Mitigation Policies.** *Chen et al.*, March 2016
293. **Uncertainty in Future Agro-Climate Projections in the United States and Benefits of Greenhouse Gas Mitigation.** *Monier et al.*, March 2016
294. **The Future of Natural Gas in China: Effects of Pricing Reform and Climate Policy.** *Zhang and Paltsev*, March 2016
295. **Are Land-use Emissions Scalable with Increasing Corn Ethanol Mandates in the United States?** *Ejaz et al.*, April 2016
296. **Statistical Emulators of Maize, Rice, Soybean and Wheat Yields from Global Gridded Crop Models.** *Blanc*, May 2016
297. **Electricity Investments under Technology Cost Uncertainty and Stochastic Technological Learning.** *Morris et al.*, May 2016
298. **Modeling Regional Carbon Dioxide Flux over California using the WRF-ACASA Coupled Model.** *Xu et al.*, June 2016